A CONTINUOUSLY VARIABLE FREQUENCY CROSS-CORRELATION PHASE FLUOROMETER WITH PICOSECOND RESOLUTION

E. GRATTON AND M. LIMKEMAN
Department of Physics, University of Illinois at Urbana-Champaign, Urbana, Illinois 61801

ABSTRACT A detailed description of the construction and performance of a variable frequency cross-correlation phase fluorometer is reported. The phase fluorometer operates over the frequency range 1–160 MHz with a maximum resolution of a few picoseconds. The effects of distortions introduced by the light modulator and the nonlinear dynode characteristic are discussed in terms of the harmonic content of the detected signal. A source of systematic errors due to nonhomogeneous modulation is also discussed with particular attention to the color effect of the photomultipliers. The application of the phase fluorometer to the measurement of very long and very short lifetimes is reported. Some application to the measurement of multiexponential decays is also illustrated.

INTRODUCTION

In recent years considerable interest has developed in the use of phase methods for the measurement of fluorescence lifetimes. The high accuracy and rapid determination of the lifetime value have frequently been considered the major advantages of this technique when compared with pulse methods. However, it was soon realized that a large number of modulation frequencies were needed to acquire the same information that is obtained by the direct recording of the time decay (1, 2). The importance of this capability has been recently emphasized (3). An application of multifrequency phase fluorometry to the measurement of oxygen quenching in proteins is reported in a companion paper (D. Jameson, E. Gratton, B. Alpert, and G. Weber, submitted for publication). The multifrequency capability of the instrument described in this report was the crucial feature for the understanding of the diffusion of oxygen in proteins. Although no continuously variable frequency phase fluorometer is commercially available, the instrument described here is made entirely of parts available on the market. It includes a laser light source, an electro-optical modulator of the laser intensity, an optical module to house the sample, photomultipliers, filters, and an electronic module for signal analysis. A detailed description of the principle and operation of the instrument is presented here together with a few selected examples. A discussion of possible artifacts in the measurements is also included.

Several descriptions of phase fluorometers have appeared in the literature (4–9). A cross-correlation phase fluorometer with subnanosecond resolution using two modulation frequencies has been reported by Spencer and Weber (10). A variable frequency instrument has been described by Haar and Hauser (11). The latter instrument uses a laser as a light source but does not make use of the cross-correlation technique. To our knowledge there have been no reports of a continuously variable frequency cross-correlation phase fluorometer. There are at least two major advantages of using the cross-correlation technique over using other phase-detection techniques. First, the low frequency part of the cross-correlation signal allows phase and modulation measurements to be performed using accurate digital methods. Second, the phase coherence of the modulation frequency and the cross-correlation frequency, as described later, nulls the phase jitter of the high frequency oscillator.

PRINCIPLE OF CROSS-CORRELATION PHASE FLUOROMETRY

The principle of operation of a cross-correlation phase fluorometer has been described by Spencer and Weber (10). When a fluoresecent probe is excited with sinusoidal intensity-modulated light of angular frequency $\omega = 2\pi f$, the emitted fluoroscence has the same frequency of modulation but is demodulated and phase-shifted with respect to the exciting light. The phase shift, ϕ, and the modulation factor, M, are related to the lifetime, τ, of the fluorescent excited state by the relations

$$\tan \phi = \omega\tau$$

$$M = M_F/M_E = 1/\sqrt{1 + (\omega\tau)^2}, \quad (1)$$

where M_F and M_E are the modulation of the fluorescence and excitation, respectively. The angular frequency ω is of the order of $1/\tau$. The emitted light intensity can be

described by the following function

$$F(t) = F_0[1 + M_F \cos(\omega t + \phi)], \quad (2)$$

where F_0 is the average fluorescence intensity. The cross-correlation method consists of multiplying the emitted function by a sinusoidal signal whose frequency, ω_c, is just slightly different from ω.

$$C(t) = C_0[1 + M_c \cos(\omega_c t + \phi_c)]. \quad (3)$$

The resulting signal is the new function

$$V(t) = F_0C_0[1 + M_F \cos(\omega t + \phi) + M_c \cos(\omega_c t + \phi_c) + M_FM_C \cos(\omega t + \phi) \cos(\omega_c t + \phi_c)]. \quad (4)$$

The last term of Eq. 4 can be rewritten by using trigonometric relationships as

$$\frac{M_FM_C}{2}[\cos(\Delta\omega t + \Delta\phi) + \cos(\omega_c t + \omega t + \phi + \phi_c)], \quad (5)$$

where $\Delta\omega = \omega_c - \omega$ and $\Delta\phi = \phi_c - \phi$. If ω_c is very close to ω, then Eq. 4 contains a constant term plus a term of frequency ω, plus a term of frequency 2ω, plus a term of frequency $\Delta\omega$. The term of frequency $\Delta\omega$ contains all the phase and modulation information of the original fluorescence signal. In the instrument described in this report, f_c has been set to 31 Hz (where $\Delta\omega = 2\pi f_c$). This low frequency component in Eq. 4 can be totally filtered from the remaining terms. In the real system both the light intensity and the electronic signal used for the cross correlation are not pure sinusoidally varying signals. The effect of the harmonic content will be discussed later.

MODULATION OF THE LIGHT INTENSITY

The overall optics and electronics layout of the fluorescence lifetime instrument is shown in Fig. 1. The light source is an argon ion laser (model 164/9; Spectra-Physics Inc., Mountain View, CA) equipped with selective prism wavelength and ultraviolet optics. Sinusoidal modulation of the light intensity is obtained with an extra-cavity electro-optical element (model IM1; Pockels cell, Lasermetrics Inc., Englewood, NJ) driven by a radio frequency (RF) power amplifier (411AL 10W; Electronic Navigation Industries Inc., Rochester, NY). As shown in Fig. 1, the light from the laser passes first through a polarizer P1 in order to increase the polarization of the laser light. This step is required due to the imperfect polarization of the laser beam and to minimize background light due to noncoherent emission from the plasma discharge of the laser tube. Furthermore, the polarization direction of the exciting light is set to 55° with respect to the horizontal direction to eliminate polarization effects in the fluorescence measurement (12). Once polarizer P1 and P2 are aligned, i.e., when the polarization plane of P1 is at 55° with respect to the laser polarization plane and P2 is perpendicular to polarizer P1, the Pockels cell is introduced between P1 and P2. The x-axis of the Pockels cell is accurately oriented at 45° with respect to the polarization plane of the polarizer P1, and the z-axis is aligned with the laser beam. The Pockels cell is mounted on a gimbal mounting such that horizontal, vertical, and rotational motions are allowed. The correct alignment of the Pockels cell is detected by the appearance of a sharp dark image after polarizer P2. This dark band moves up and down as an alternating voltage is applied to the Pockels cell. The driver circuit is shown schematically in Fig. 2. The 25 W 50Ω resistor R1 is placed as close as possible (~2 cm) to the Pockels cell to minimize the length of the mismatched transmission line. A biasing circuit is used, consisting of a decoupling capacitor, C, a protection resistor, R2, and an inductor, L. The inductor prevents the RF signal from reaching the input of the direct current (DC) voltage source. The RF power at the output of the amplifier is

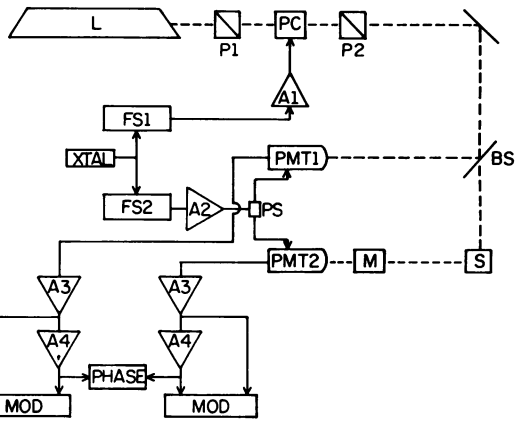

FIGURE 1 Block diagram of the instrument. *L*, argon ion laser (model 164/9; Spectra Physics Inc.); *P1*, *P2*, Glan-Thompson UV polarizers; *PC*, Pockels cell (LM1; Lasermetrics, Inc., Englewood, NJ); *BS*, quartz beam splitter 1/100; *FS1*, frequency synthesizer (5600; Rockland Systems, Co.); *FS2*, frequency synthesizer (6160A; Fluke, John, Mfg. Co., Inc.); *XTAL*, 5 MHz quartz crystal; *A1*, 10-W RF power amplifier (411AL; ENI Power Systems, Inc., Rochester, NY); *A2*, 2-W power amplifier (502C; RF Power Labs); *PS*, power splitter (model PD-20-50M2; Merrimac Industries, Inc., West Caldwell, NJ); *S*, sample; *M*, ¼ meter monochromator (Jarrel-Ash Div., Fisher Scientific, Co.); *PMT1*, *PMT2*, photomultipliers (R928; Hamamatsu Corp.); *A3*, DC amplifier (SLM Inc.); *A4*, AC tuned amplifier (SLM Inc.); *PHASE*, phase meter (SLM Inc.); *MOD*, digital ratio voltmeter (SLM Inc.).

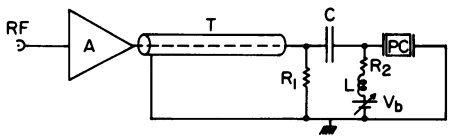

FIGURE 2 Pockels cell driving circuit. *A*, 10-W RF power amplifier (411 AL; ENI Power System, Inc.); *C*, 0.1 μF, 500-V ceramic capacitor; *L*, 500-μH inductor; *PC*, Pockels cell (Lasermetrics Inc.); *R1*, 50Ω, 25-W power coaxial resistor (8085; Bird Electronic Corp.); *R2*, 5 KΩ, ¼-W resistor; *T*, 50Ω coaxial transmission line (58A/U; RG Circuits Co., Escondido, CA); V_b, 0–200 V voltage source (Kepco, Inc., Flushing, NY).

monitored with a wattmeter (model 4430; Bird Electronic Corp., Cleveland, OH). Usually the power output is kept between 5 and 10 W over all the frequency range 1.0–160 MHz. The peak-to-peak voltage at the Pockels cell can be calculated from the measured power, P, as

$$V_p = 2.8 \times (P \times R_l)^{1/2}. \quad (6)$$

This voltage is in the range 45–65 V. The light intensity as measured by the reference photomultiplier as a function of the biasing voltage, V_b, is shown in Fig. 3. The biasing voltage, V_b, is chosen so that the modulation frequency is equal to the RF driving frequency. V_b is therefore set to a value between 50 and 70 V. At very low voltage there is a slight deviation from the quadratic law (not visible in Fig. 3). The reason for this deviation can be qualitatively understood if the optical system is considered. Suppose for example that the dark band moves up, so that the upper part is dark but the lower part is bright, when the band moves down the opposite occurs. The net result is a decrease in the overall modulation. Furthermore the modulated intensity will be the sum of two sinusoidal modulated signals spatially separated and with opposite phase. If the detection system is not perfectly independent of the geometry of the beam, quite dramatic effects can occur. These will be discussed later in the section on systematic errors. We choose the biasing voltage such that the dark band is always in the upper or lower part of the laser beam as the alternating voltage is applied. The modulated light beam is sent to the entrance of an optical module (model OP450; SLM Inc., Urbana, IL). Fig. 4 shows schematically the optical path. The incoming beam is split (1:100) by a quartz plate and a fraction of the beam is sent to a scattering cuvette. The scattered light is detected by the reference photomultiplier (PMT3; Hamamatsu Corp., Middlesex, NJ). A neutral density filter in filter holder F1 can be used to attenuate this beam. The reference signal is normally used as a reference for the phase signal only. The

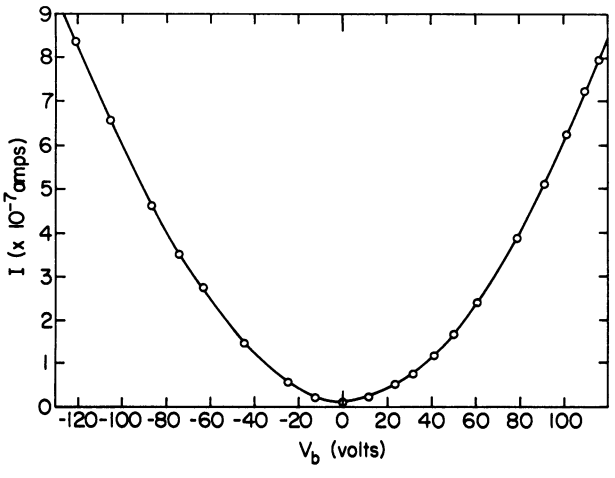

FIGURE 3 Pockels cell characteristic curve.

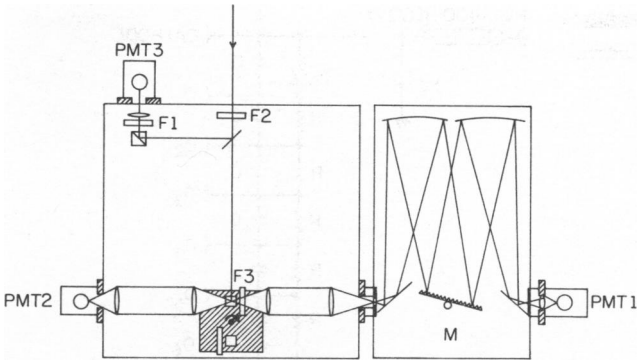

FIGURE 4 Schematic diagram of the optics. *F*1, *F*2, *F*3, filter holders; *M*, ¼ meter grating monochromator (Jarrell-Ash Div., Fisher Scientific Co.); *PMT*1, *PMT*3, photomultipliers (R928; Hamamatsu Corp.); *PMT* 2, photomultiplier (2230; Amperex Electronic Corp.); *T*, rotating turret.

total beam can be attenuated by a neutral density filter in filter holder F2. A fluorescent sample and a scattering sample (polystyrene) are placed in a rotating turret. A filter is generally inserted in filter holder F3 in order to strongly attenuate the scattered laser intensity. When the scattering solution is in position, the filter rotates with the turret. The emitted or scattered light is collected by a lens system and focused on the entrance slit of a ¼ meter grating monochromator (Jarrell-Ash Div., Fisher Scientific Co., Waltham, MA). The bandwidth of this monochromator is generally fixed at 3.3 nm. The monochromator is mounted vertically so that the slits are parallel to the laser beam. This enhances the collection of the emitted light. At the monochromator output a lens and a diaphragm are used to focus the beam on a small area of the sample photomultiplier, PMT 1.

PHOTOMULTIPLIER CIRCUIT

At the present time we have three photomultipliers installed on the instrument. One photomultiplier, Hamamatsu R928 (Hamamatsu Corp.), is used in the reference arm. An identical photomultiplier is used in the right arm of the optical module. The third photomultiplier, Amperex 2023 (Amperex Electronic Corp., Slatersville, RI), is used in the left arm. The choice of these phototubes has been dictated by their wavelength sensitivity, their frequency response, and their color effect (see section on systematic errors). The Hamamatsu R928 photomultiplier (Hamamatsu Corp.) is a red sensitive tube with good frequency response and virtually no color effect. The Amperex 2023 photomultiplier (Amperex Electronic Corp.) is a high sensitivity tube with excellent response in the blue, good frequency response and very little color effect. In the past two years we have used mainly the Hamamatsu R928 tube (Hamamatsu Corp.) because of the red sensitivity and because of the low voltage required for the RF modulation. The photomultiplier circuit for this tube is shown in Fig. 5. It is composed of a linear chain divider and a circuit for the RF modulation. The modulation is obtained by applying an

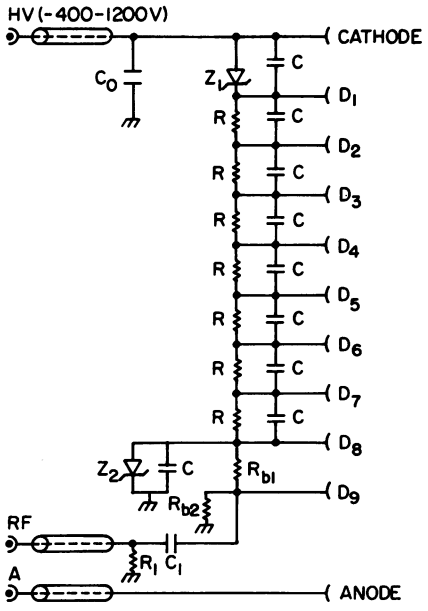

FIGURE 5 Photomultiplier dynode circuit. *A*, anode output; *C*, 500 pF, 1-kV ceramic capacitor; *C*, 1,000 pF, 6 kV ceramic capacitor; C_1, 0.1 μF, 500-V ceramic capacitor; *D1–D9*, dynodes; *HV*, 0–1,200-V high voltage source; *R*, 500 KΩ ¼-W resistor; R_1, 50Ω, 2-W resistor; R_{b1}, 5MΩ ¼-W resistor; R_{b2}, 20 KΩ ¼-W resistor; *RF*, radio frequency signal input; *Z1*, SK 3427 zener diode; *Z2*, 1N 4761 zener diode.

alternating voltage to the last dynode, D_9. In Fig. 6 we report the output current at the anode under the condition of constant cathode illumination as a function of the voltage applied to the last dynode. It can be seen that a voltage of −4 V is necessary to turn off the tube. The characteristic curve has a sharp rise for small voltages and then the current reaches a maximum and decays slowly as the voltage at the dynode increases. The part of the characteristic curve between −4 to +10 V is used to modulate the tube. A resistor network composed of R_{b1} and R_{b2} is used to bias the last dynode at 0.2 V. This is approximately the center of the linear part of the characteristic. A capacitor, C_1, is used to decouple the biasing voltage from the RF signal. The characteristic curve depends on the voltage at the dynode D_8. A zener diode, Z2, is used to maintain this voltage constant. Notice that at low voltage the characteristic is not linear. This nonlinearity introduces a distortion of the modulation signal that is reflected in the harmonic content at the photomultiplier output. We will discuss this point later. The voltage range necessary to vary the output current of the photomultiplier by 90% is ~10 volts. This value corresponds to a power of 0.25 W on 50Ω. This voltage is provided by an RF amplifier (model M 502C, RF Power Labs Inc., Woodinville, WA). The amplifier can deliver up to 2 W. A zener diode, Z1, is used to maintain a constant voltage between the cathode and the first dynode. The color effect depends on the acceleration voltage for the emitted electrons at the photocathode. The higher this voltage is the smaller the color effect. The value of the zener diode has been chosen in order to have the maximum acceleration voltage compatible with the tube specifications.

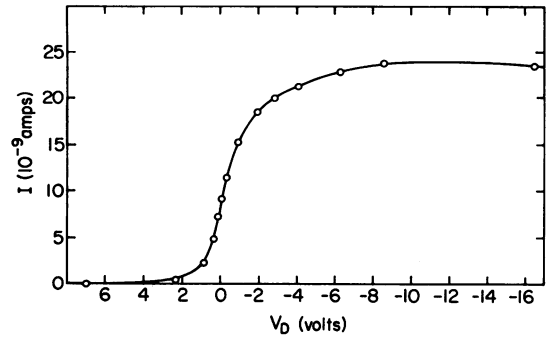

FIGURE 6 Dynode characteristic curve.

ELECTRONIC DETECTION SYSTEM

The outputs of the reference and sample photomultipliers are sent to the electronic detection system for analysis. Two identical channels are used for the reference and sample signals. Each channel is composed of a DC and an alternating current (AC) amplifier. The amplifiers are commercial modules purchased from SLM/AMINCO Inc. (Urbana, IL). Two outputs are available at the DC amplifier, (*a*) a low impedance sinusoidal signal used as an input for the AC amplifier, and (*b*) an integrated signal sent to a digital voltmeter. This DC signal is proportional to the average intensity. We will call this signal the DC voltage. The AC amplifier is a narrow band amplifier tuned at 31 Hz with a *Q* of ~200 (Fig. 7). The AC amplifier has three outputs. The first corresponds to the sinusoidal filtered signal at 31 Hz to be used with a digital phase-sensitive detector

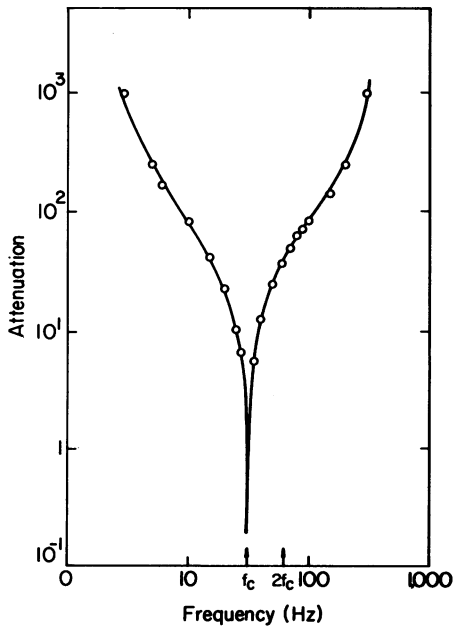

FIGURE 7 AC filter response curve. The filter is tuned at 31 Hz.

described in a separate paper (E. Gratton and R. Hall, manuscript in preparation). The second output is the rectified value of the AC signal and is sent to a digital voltmeter. In the following this voltage will be referred to as the AC voltage. The third output is a square wave generated by the zero crossing of the AC signal. This signal is sent for the phase measurement. The voltage corresponding to the average value of the DC signal and the voltage corresponding to the rectified value of the AC signal are measured by an integrating digital voltmeter. This voltmeter can be used to measure the DC signal, the AC signal, or the AC/DC ratio. The AC/DC ratio is also called the modulation of the signal.

CROSS-CORRELATION FREQUENCY GENERATION

The signals for the modulation of the light and for the modulation of the photomultipliers are generated by two frequency synthesizers. One is a model 5600 from the Rockland Systems Co. (Rockleigh, NJ) and the second from John Fluke Mfg. Co., Inc. (model 6160A; Everett, WA). Both frequency synthesizers have a frequency range from 1 to 160 MHz and a resolution of 1 Hz. The Rockland Systems Corp. synthesizer is locked to the same quartz crystal as the John Fluke Mfg. Co., Inc. synthesizer, so that the signals are coherent in phase over all the frequency range. The phase noise, which is the only important parameter in this configuration, has been checked by setting the two generators at 100,000,000 and 100,000,001 Hz for both synthesizers. The two outputs were sent to a mixer (model ZAD1; Mini-Circuits Lab, Brooklyn, NY) and the period of the wave at 1 Hz was measured. The period was constant within 4 significant digits using an integration time of 1 s. The corresponding phase noise was estimated to be <0.036°. No drift was observed over a period of 2 h. Note that the two synthesizers are not equipped with the high stability crystal option, an unnecessary feature since only the phase coherence of the two synthesizers to the same crystal is important to us.

The system described can work in the frequency range 1–160 MHz, the limits being imposed by the range of the synthesizers. However some other factors limit the maximum operating frequency as well. At very high frequency, around 150 MHz, a degradation of the modulation is observed. Also around 120 MHz a decrease of modulation is noticed. These effects are due to the light modulator. The Pockels cell dissipates heat at high frequency and shows some sort of resonance at 120 MHz. Another identical Pockels cell was also tested but similar results were obtained. The photomultiplier also attenuates the signal at high frequency. The rise time of the Hamamatsu R928 (Hamamatsu Corp.) is 2.2 ns. This value corresponds to an effective bandwidth of 160 MHz. In Fig. 8 we report the normalized frequency response of the system. The modulation was measured for a scattering solution. The biasing voltage at the Pockels cell was set to 50 V. The RF power at the light modulator was 5 W at 10 MHz. For the results reported in Fig. 8 no adjustment of the biasing voltage of the Pockels cell was done. The only variable was the frequency of the synthesizers. Higher modulation values at high frequency can be obtained if the biasing voltage at the Pockels cell is decreased.

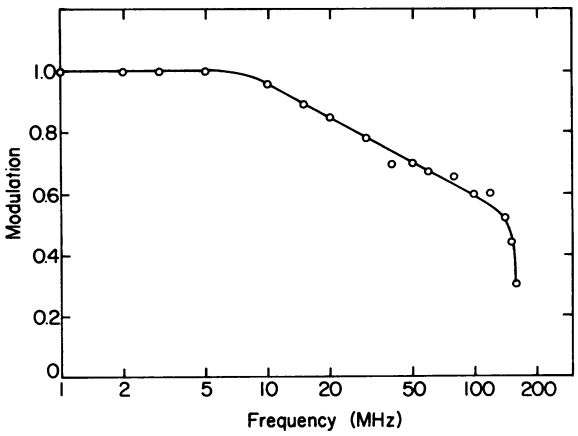

FIGURE 8 Normalized overall frequency response of the instrument.

ANALYSIS OF THE HARMONIC CONTENT

It is important to analyze the signals generated in the instrument in order to understand the response of the system to distortions introduced by the intrinsic nonlinear elements of the circuit, namely, the Pockels cell and the dynode characteristic, and to demonstrate the negligible influence of these distortions on the lifetime measurement.

The response of the light modulator can be approximated by a quadratic function for low biasing voltages (see Fig. 3) as

$$I(t) = I_0 \sin^2 V_b/V_0 \simeq I_0(V_b/V_0)^2. \tag{7}$$

The biasing voltage has the following expression, $V_b = V_b^0 + m \sin(\omega t + \phi)$, where V_b^0 is the DC biasing voltage and m is the amplitude of the AC signal at the output of the RF amplifier. V_0 is characteristic of the Pockels cell. Assume that $\phi = 0$ in the following and that no distortions are introduced by the RF amplifier. The modulated light intensity from the Pockels cell can be described by the following function

$$I(t) = \frac{I_0}{V_0^2}\left[(V_b^0)^2 + \frac{m^2}{2} + 2\,V_b^0\, m \sin \omega t + \frac{m^2}{2}\cos 2\,\omega t\right]. \tag{8}$$

This function contains three terms, with frequencies 0, ω, and 2ω. The modulation of the light intensity is defined by the ratio of the amplitude of the term of frequency ω to the DC part, $M_E = 2\,V_b^0\, m/[(V_b^0)^2 + m^2/2]$. The maximum value of the modulation is $\sqrt{2}$ for $m/V_b^0 = \sqrt{2}$. Each individual component at frequency ω and 2ω is attenuated

and phase shifted by the fluorescence sample. The fluorescence signal at the photomultiplier due to the emitted light has the form

$$F(t) = F_0\left[1 - \sum_k f_k \cos(k\omega t + \phi_k)\right] \qquad k = 1, 2. \quad (9)$$

The cross-correlation signal for the modulation of the photomultiplier current will be described by a similar expression

$$C(t) = C_0\left[1 - \sum_l f_l^c \cos(l\ \omega_c t + \phi_l^c)\right] \quad l = 1, 2 \ldots . \quad (10)$$

The harmonic content of $C(t)$ is greater than that of the fluorescence signal because of the highly nonlinear characteristic of the photomultiplier dynode. At the output of the photomultiplier the waveform will be

$$V(t) = F(t) \cdot C(t) = F_0C_0\left[1 - \sum_k f_k \cos(k\omega t + \phi_k)\right] \times \left[1 - \sum_l f_l^c \cos(l\,\omega_c t + \phi_l^c)\right]. \quad (11)$$

The average value of V is given by

$$V_{DC} = F_0C_0. \quad (12)$$

This voltage constitutes the DC signal.

To calculate the lowest frequency we notice that the difference between ω and ω_c is the cross-correlation frequency, $f_c = 31$ Hz. The lowest frequency term is obtained for $k = 1, l = 1$.

$$V_{AC} = F_0C_0f_1f_1^c \cos(2\pi f_c t + \phi_1 - \phi_1^c). \quad (13)$$

This is the only term giving a frequency f_c. All other combinations for different values of k and l give a frequency of $2f_c$ or greater. The response curve of the AC filter is reported in Fig. 7. This filter rejects the frequency $2f_c$ with respect to f_c by a factor of 200. This analysis demonstrates that the distortions introduced by the nonlinearity in the modulation of the light and in the modulation of the photomultiplier do exist, but have a negligible effect on the measurements since the filter will reject them. The expression derived for the AC and DC signals can be used to calculate the theoretical value of the AC/DC ratio for a scattering sample.

$$(AC/DC)_{scatt} = f_1f_1^c. \quad (14)$$

This expression shows that to achieve a high AC/DC ratio both f_1 and f_1^c must be as large as possible. In general, f_1 and f_1^c are close to one over the entire frequency range. This analysis also shows that a high frequency pulsed light source with a large harmonic content is as well suited for cross-correlation phase fluorometry as a sinusoidally modulated source (13, 14).

SENSITIVITY OF THE PHASE FLUOROMETER

In a typical measurement, phase and modulation values are obtained for a scattering and a fluorescent sample. For the chosen photomultiplier tubes and amplifiers, these quantities can be measured for fluorescence intensities as low as a few thousand photons per second. The phase of the fluorescence with respect to the scattering is defined as

$$\phi = (\phi_{1,F} - \phi_{1,F}^c) - (\phi_{1,S} - \phi_{1,S}^c), \quad (15)$$

where ϕ_1 and ϕ^c have been previously defined. The suffixes F and S indicate fluorescent and scatter samples, respectively. In general, $\phi_{1,F}^c$ and $\phi_{1,S}^c$ are identical since they are electronic delays. They would be different in the case of drift of the electronic phase. The modulation of the fluorescence is defined as

$$M = (AC/DC)_F/(AC/DC)_S, \quad (16)$$

where the ratio AC/DC has been previously defined.

The phase angle is measured in degrees with a resolution of 0.01° over the entire frequency range (1 to 160 MHz) for a 20-s integration time. The noise in the phase measurement depends on many factors, the major one being the signal intensity. Generally the standard deviation for a series of ten phase measurements in typical signal conditions is on the order of 0.05–0.10°. Phase drifts over a long period of time, and systematic errors are generally greater than phase noise. Phase drifts can be taken into account by alternating measurements of the phase delay for the scattering and fluorescent sample. Over a period of 6 h the phase drift is <1°. Systematic errors in the phase values will be discussed later. However, taking into account only phase noise, the resolution in phase at a frequency of 100 MHz corresponds to an actual lifetime resolution on the order of 2–3 ps. This is the minimum lifetime difference that can be detected with this instrument using phase measurements.

The modulation is a ratio of two voltages. The accuracy in the determination of the modulation is 10^{-3}. In normal signal conditions the standard deviation for a series of two modulation measurements is 2×10^{-3}. Modulation drifts are larger than phase drifts. Modulation drifts of 10^{-2} over a period of 6 h have been noticed. Systematic errors in the determination of the modulation values will be discussed in the next section. Considering only modulation measurements the minimum lifetime difference that can be detected is 5 ps at 100 MHz. Note here that we are considering lifetime differences at maximum modulation sensitivity. When other than ideal conditions occur, the sensitivity of the measurement decreases (13).

SYSTEMATIC ERRORS IN THE DETERMINATION OF PHASE AND MODULATION VALUES

In our experience with phase fluorometry for the past several years we have found at least two different kinds of

systematic errors that can give rise to dramatic effects on the measured values of phase and modulation. The first error, due to nonhomogeneous modulation of the light beam, can give rise to completely erratic data. This effect can be particularly large for acousto-optic modulators. It is our opinion that this effect has been largely neglected in considering possible artifacts in lifetime measurements by phase fluorometry. The nonhomogeneous modulation effect is strongly reduced in the electro-optical light modulator used in this report. The second effect depends on the wavelength-dependent phase delay due to the different kinetic energies of the emitted electrons at the photocathode. This color effect has been extensively discussed (2, 15–18). It can be minimized by using a reference substance of known lifetime with emission at the same wavelength as that of the sample to be measured.

To illustrate the origin of these two systematic errors consider a light beam of a given cross section and suppose the modulation of the beam is nonhomogeneous in both phase and amplitude. For example suppose one component of the beam has a time dependence, $A(t)$, and the other component a similar time dependence, $B(t)$, where

$$A(t) = A_0[1 + m_A e^{j(\omega t - \phi_0)}] \tag{17}$$

$$B(t) = B_0(1 + m_B e^{j\omega t}). \tag{18}$$

In these expressions A_0 and B_0 are the DC intensities of the two parts of the beam, m_A and m_B are the modulations of the two regions, ϕ_0 is the phase delay of A with respect to B, and ω is the circular frequency of modulation. A, B, m_A, m_B, and ϕ_0 can represent either two different geometrical parts or two different wavelength regions of the light beam, or represent both simultaneously. The separation of the beam into two different regions is arbitrary. In no experimental situation will the beam be divided into exactly two parts; the simplification is used here only to calculate the kind of effects that can be expected from the nonhomogeneous modulation of the beam. The geometrical and/or wavelength separation of the two regions of the beam can cause different samples to weight more or less the contribution to the measured phase and modulation of one part of the beam with respect to the other. For example a scattering sample with a relatively large optical thickness can have a geometrical and wavelength distribution of the scattered light different than that of a weakly absorbing fluorescent sample. For a real experimental system the effect is quite unpredictable, depending on the particular geometry of the experiment, on the sensitivity of different areas of the photomultiplier, on the position of the absorption band of the fluorescent sample, etc. For the two-component simplification the effect of this nonhomogeneous modulation on the phase measurement can be calculated. The excitation light is the sum of the contributions of part A and B of the beam. Because each part is assumed to behave independently, the total fluorescent emission is

$$F(t) = F_A + F_B = F_{0A}[1 + m_{FA}e^{j(\omega t - \phi_{FA})}] + F_{0B}[1 + m_{FB}e^{j(\omega t - \phi_{FB})}], \tag{19}$$

where

$$\phi_{FA} - \phi_0 = \tan^{-1}\omega\tau; \quad \phi_{FB} = \tan^{-1}\omega\tau$$

$$\frac{m_{FA}}{m_A} = \frac{1}{\sqrt{1 + \omega^2\tau^2}}; \quad \frac{m_{FB}}{m_B} = \frac{1}{\sqrt{1 + \omega^2\tau^2}}. \tag{20}$$

τ is the lifetime of the probe, assumed to be homogeneous. The phase and modulation of the excitation wave due to the sum of $A(t)$ and $B(t)$ is

$$\phi_{EX} = \tan^{-1}\frac{\sin\phi_0}{\cos\phi_0 + R_0}$$

$$m_{EX} = \sqrt{1 + R_0^2 + 2R_0\cos\phi_0}\,\frac{A_0 m_A}{A_0 + B_0}, \tag{21}$$

where

$$R_0 = \frac{B_0 m_B}{A_0 m_A}. \tag{22}$$

The phase of the emitted wave is

$$\phi_{EM} = \tan^{-1}\left(\frac{\sin\phi_{FA} + R_F\sin\phi_{FB}}{\cos\phi_{FA} + R_F\cos\phi_{FB}}\right) \tag{23}$$

where

$$R_F = \frac{F_{0B}m_{FB}}{F_{0A}m_{FA}}. \tag{24}$$

If ϕ_0 is zero or $\phi_0 = \pi$ (i.e., the two parts of the beam are in phase or out of phase one with respect to the other), then the phase of the emission is unperturbed. If $R_0 = 0$ clearly the beam is homogeneous and the phase is unperturbed. The measured quantity is the difference between the emission and excitation.

$$\phi = \phi_{EM} - \phi_{EX}. \tag{25}$$

Using the expressions for ϕ_{FA} and ϕ_{FB} in terms of τ this expression becomes

$$\phi = \tan^{-1}\omega\tau + \tan^{-1}\frac{\sin\phi_0}{\cos\phi_0 + R_F} - \tan^{-1}\frac{\sin\phi_0}{\cos\phi_0 + R_0}. \tag{26}$$

If $R_F = R_0$ then $\phi = \tan^{-1}\omega\tau$. This is the expected result if no difference in the heterogeneity of the modulation occurs between emission and excitation. Notice that the angle added by nonhomogeneous modulation is independent of the frequency. This angle can be positive or negative and quite large.

The value of the modulation can also be calculated in the presence of the nonhomogeneous modulation. The modula-

tion of the emitted light is

$$M_{EM} = \sqrt{1 + R_F^2 + 2R_F \cos(\phi_{FA} - \phi_{FB})}\,\frac{F_{0A}m_{FA}}{F_{0A} + F_{0B}}. \quad (27)$$

The ratio of the modulation of the emission to the modulation of the excitation is

$$M = \frac{M_{EM}}{M_{EX}} = \frac{1}{\sqrt{1 + \omega^2\tau^2}} \sqrt{\frac{1 + R_F^2 + 2R_F \cos\phi_0}{1 + R_0^2 + 2R_0 \cos\phi_0}}\,\frac{F_{0A}(A_0 + B_0)}{A_0(F_{0A} + F_{0B})}. \quad (28)$$

The correction factor multiplying the modulation can be larger or smaller than one. The expressions given above for ϕ and M can be easily generalized to the case of dividing the exciting beam into more than two parts.

To calculate the magnitude of the effect of the nonhomogeneous modulation on the measured values of lifetime by phase and modulation, consider the following example. Suppose we are measuring the fluorescence emitted by a sample with a characteristic lifetime τ at a circular modulation frequency $\omega = 2\pi f$. Let us assume the incident beam is made of two parts, one part A of light in the absorption band of the probe and one part B of light not in the absorption band of the fluorescent molecule. The total incident light is

$$S = A_0[1 + m_A e^{j(\omega t - \phi_0)}] + B_0(1 + m_B e^{j\omega t}), \quad (29)$$

where we assume that A and B have different modulations and different phases. Using the expressions derived above, the phase and modulation of the excitation are

$$\phi_{EX} = \tan^{-1}\frac{\sin\phi_0}{\cos\phi_0 + R_0}$$

$$M_{EX} = \sqrt{1 + R_0^2 + 2R_0\cos\phi_0}\,\frac{A_0 m_A}{A_0 + B_0}. \quad (30)$$

The emitted light, due only to the part A of the incident beam, has phase and modulation

$$\phi_{EM} = \tan^{-1}\omega\tau$$

$$\frac{m_{EM}}{m_A} = \frac{1}{\sqrt{1 + \omega^2\tau^2}}. \quad (31)$$

The measured values of the phase and modulation are

$$\phi = \tan^{-1}\omega\tau - \tan^{-1}\frac{\sin\phi_0}{\cos\phi_0 + kl}$$

$$M = \frac{1}{\sqrt{1 + \omega^2\tau^2}}\sqrt{\frac{(1 + k)^2}{1 + k^2l^2 + 2kl\cos\phi_0}}, \quad (32)$$

where $k = B_0/A_0$ and $l = m_B/m_A$. In Fig. 9 we report the evaluation of the measured lifetime for two different values of τ and two pairs of values of k and l as a function of the phase angle between the two parts of the incident light beam. In these calculations the frequency is 30 MHz. Two different probes with lifetimes 3 and 30 ns have been used. From these simulations it can be seen that nonhomogeneous modulation can give a completely erratic result in the measured lifetime values. Notice that the values we have chosen for k and l are quite reasonable in normal experimental conditions. This simulation also shows that the absolute uncertainty due to systematic errors in the measurement of the lifetime value can be much larger than the relative noise associated with a single measurement. If no particular attention is given to avoiding the nonhomogeneous modulation artifact, the absolute lifetime values obtained by phase fluorometry have no meaning at all. We mention again that this effect has been largely neglected.

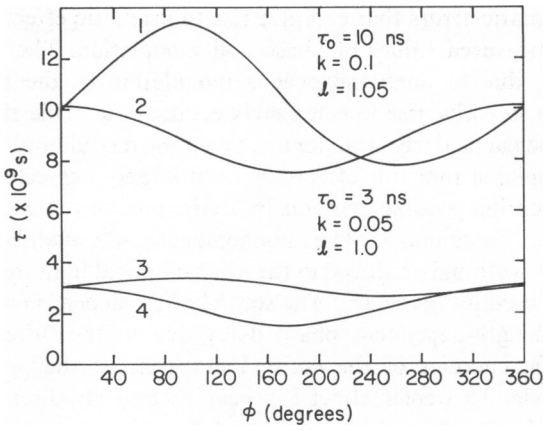

FIGURE 9 Calculated apparent lifetime by phase and modulation due to nonhomogeneous modulation artifact. Curve 1 and 3 lifetime by phase. Curve 2 and 4 lifetime by modulation. The frequency of modulation is 30 MHz.

The same equations can be used to calculate the color effect. In this case the part B of the beam is zero but ϕ_0 is wavelength dependent so that the scattering sample and the fluorescent sample have a different ϕ_0. In this particular condition the measured phase and modulation are

$$\phi = \tan^{-1}\omega\tau - \phi_0$$

$$M = \frac{1}{\sqrt{1 + \omega^2\tau^2}}. \quad (33)$$

The phase value only is perturbed in this case. This is clearly a particular case of a more general color effect. In fact not only ϕ_0 but also A_0, B_0, and m_A, m_B as well can be wavelength dependent. In this case a more complex color effect is present and both phase and modulation values can equally well be effected.

APPLICATIONS OF THE PHASE FLUOROMETER

In this section some applications of the phase fluorometer for the measurement of the lifetime of fluorescent samples

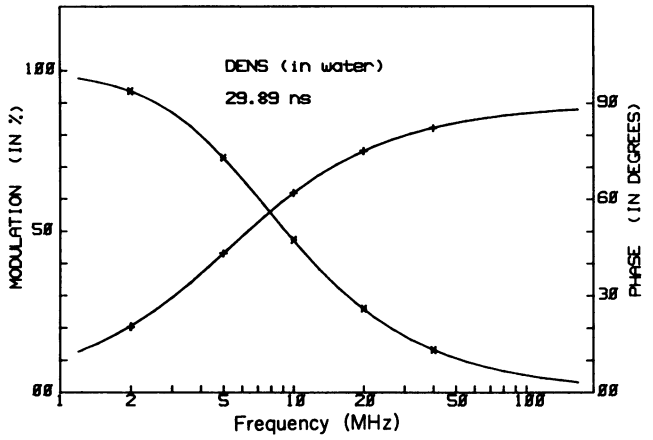

FIGURE 10 Phase (+) and modulation (*) values as a function of frequency for DENS in water. The solid lines (—) correspond to the best fit of the data using a nonlinear least-squares routine for a single exponential component of lifetime τ = 29.86 ns.

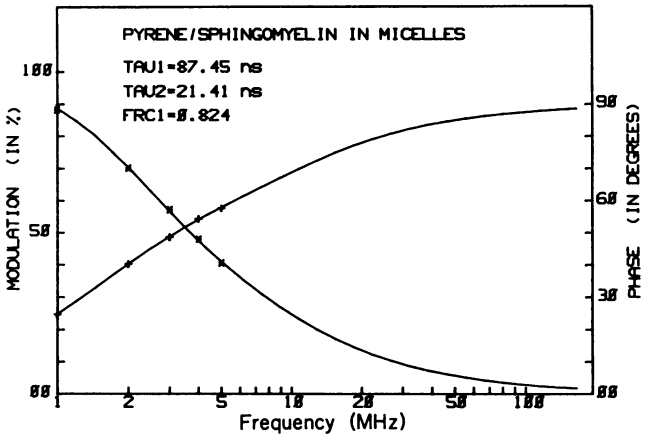

FIGURE 12 Phase (+) and modulation (*) values as a function of frequency for pyrene covalently bound to sphingomyelin in micelles. The solid lines (—) correspond to a two-exponential component best fit of the data with lifetimes τ_1 = 87.45 ns and τ_2 = 21.41 ns having fractional amplitudes f_1 = 0.824 and f_2 = 0.176.

are reported. In the accompanying paper (D. Jameson, E. Gratton, B. Alpert, and G. Weber, submitted for publication) a detailed analysis of the application of the phase fluorometer to an important biological problem is presented. To illustrate in this paper some applications of this new technique, we choose some extreme cases: (*a*) a sample with a long single exponential lifetime, (*b*) a probe with a very short single exponential lifetime, (*c*) a case of double exponential decay where the two components are very long lived, and (*d*) a system with a multiexponential decay where the components have a very short lifetime.

(*a*) The lifetime of an aqueous solution of DENS (2-diethylamino-5-naphthalene sulfonic acid) is measured over the frequency range 2–40 MHz. The sample is excited at 351 nm and the fluorescence is measured at 480 nm with 3.3 nm bandwidth. The measured phase and modulation values are reported in Fig. 10. An analysis of the phase and modulation data was performed using the nonlinear least-squares routine described elsewhere.[3] A lifetime value of 29.89 ns using a single exponential component was obtained. The relatively long lifetime of DENS will amplify color effects at the high modulation frequencies. The fact that no phase lengthening was detected at high frequency points out that in this configuration the color effect is negligible. A color effect of 10 ps should be easily detectable at 40 MHz for DENS. In fact the apparent lifetime by phase if a 10 picosecond color effect is added should be 32 ns at that frequency. We measured 29.9 ± 0.2 ns. (b) The lifetime of POPOP *p*-bis(2-[5-phenyloxazolyl]) benzene in ethyl alcohol was measured over the frequency range 1–140 MHz. The excitation was at 351 nm and the emission at 420 nm. The phase and modulation data are reported in Fig. 11. For this sample a single exponential

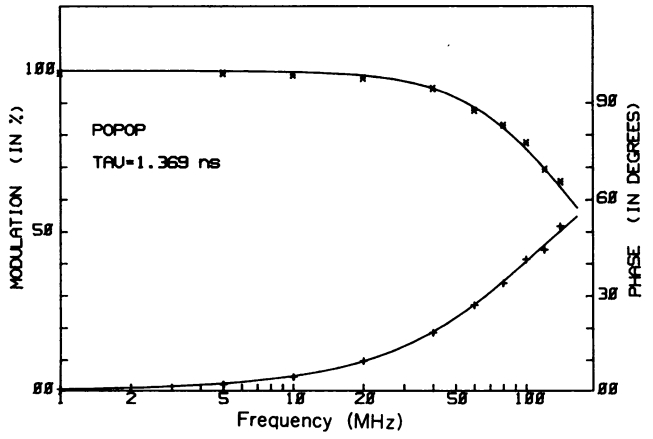

FIGURE 11 Phase (+) and modulation (*) values as a function of frequency for POPOP in ethyl alcohol. The solid lines (—) correspond to the best fit of the data with a single exponential component of lifetime τ = 1.37 ns.

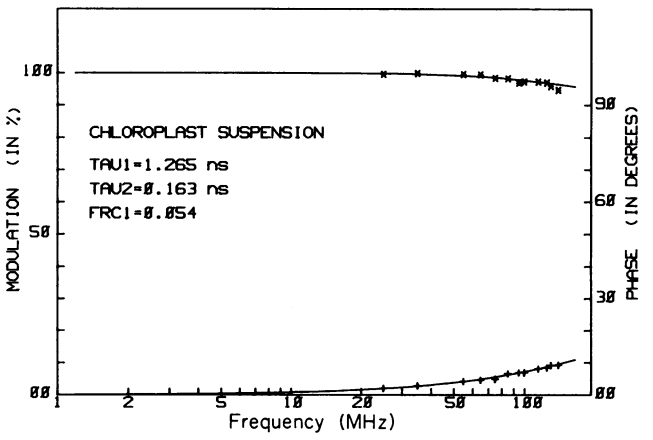

FIGURE 13 Phase (+) and modulation (*) values as a function of frequency for a chloroplast suspension from maize. The solid lines (—) correspond to a two-exponential best fit of the data with lifetimes τ_1 = 1.265 ns and τ_2 = 0.163 ns having fractional amplitudes f_1 = 0.054 and f_2 = 0.946.

decay with a characteristic time of 1.37 ns fits the data. For such a short lifetime color effects should be undetectable. (*c*) The lifetime of a pyrene derivative covalently bound to the nonpolar head of sphyngomyellin (in micelles) was measured over the frequency range 1–5 MHz. The excitation was at 351 nm and the emission at 374 nm. The values of phase and modulation as a function of the frequency are reported in Fig. 12. The least-squares analysis clearly shows the existence of two exponential components of 87 and 21 ns with fractional amplitude of 0.82 and 0.18, respectively. (d) As a final example of a measurement of a short lifetime the decay of a chloroplast suspension from maize was measured. The phase and modulation values are reported in Fig. 13. The excitation was at 488 nm and the emission at 705 nm. For this sample the emission follows a quite complex pattern. The apparent lifetime by phase depends on the emission wavelength. Furthermore the analysis using only to exponential components fails to give a satisfactory fit over all the emission band.

We would like to thank Dr. J. Lakowicz, Dr. Parkson Chong, and Mr. James Fenton for the samples used to illustrate the fluorometer's operation. Special gratitude goes to G. Weber who inspired this work.

We would like to acknowledge the financial support of the National Science Foundation grant PCM 79-18646, the Biomedical Research Support Grant PHS-2-507-RR07030-16, and a Cottrel Grant from the Research Corporation for the work reported in this article.

Received for publication 4 January 1983 and in final form 8 June 1983.

REFERENCES

1. Weber, G. 1981. Resolution of the fluorescence lifetimes in a heterogeneous system by phase and modulation measurements. *J. Phys. Chem.* 85:949–953.
2. Jameson, D. M., and G. Weber. 1981. Resolution of the pH-dependent heterogeneous fluorescence decay of tryptophan by phase and modulation measurements. *J. Phys. Chem.* 85:953–958.
3. Jameson, D. M., and E. Gratton. 1983. Analysis of heterogeneous emissions by multifrequency phase and modulation fluorometry. *In* New Directions in Molecular Luminescence. D. Eastwood and L. Cline-Love, editors. American Society for Testing and Materials. 67–81.
4. Gaviola, E. Z. 1927. Ein Fluorometer. Apparat zur Messung von Fluoreszenzabklingungszeiten. *Z. Physik.* 42:852–861.
5. Birks, J. B., and D. J. Dyson. 1961. Phase and modulation fluorometer. *J. Sci. Instrum.* 38:282–285.
6. Muller, A., R. Lumry, and H. Kokubun. 1965. High performance phase fluorometer constructed from commercial subunits. *Rev. Sci. Instrum.* 36:1214–1226.
7. Bailey, E. A., and G. K. Rollefson. 1953. The determination of the fluorescence lifetimes of dissolved substances by a phase shift method. *J. Chem. Phys.* 21:1315–1326.
8. Menzel, E. R., and Z. D. Popovic. 1978. Picosecond-resolution fluorescence lifetime measuring system with a cw laser and a radio. *Rev. Sci. Instrum.* 49:39–44.
9. Gugger, H., and G. Calzaferri. 1980. Picosecond time resolution by a continuous wave laser amplitude modulation technique. II. Experimental basis. *J. Photochem.* 13:295–307.
10. Spencer, R. D., and G. Weber. 1969. Measurements of subnanosecond fluorescence lifetime with a cross-correlation phase fluorometer. *Ann. NY Acad. Sci.* 158:361–376.
11. Haar, H. P., and M. Hauser. 1978. Phase fluorometer for measurement of picosecond processes. *Rev. Sci. Instrum.* 49:632–633.
12. Spencer, R. D., and G. Weber. 1970. Influence of brownian rotations and energy transfer upon the measurements of fluorescence lifetime. *J. Chem. Phys.* 52:1654–1663.
13. Gratton, E., and R. Lopez-Delgado. 1980. Measuring fluorescence decay times by phase-shift and modulation techniques using the high harmonic content of pulsed light sources. *Nuovo Cimento B.* 56:110–124.
14. Sabersky, A. F., and I. H. Munro. 1978. Picosecond phase shift measurements at 358 MHz using synchrotron radiation. *In* Picosecond Phenomena. C. V. Shank, editor. Springer-Verlag, New York Inc., New York. 85–88.
15. Lakowicz, J. R., H. Cherek, and A. Balter. 1981. Correction of timing errors in photomultiplier tubes used in phase-modulation fluorometry. *J. Biochem. Biophys. Methods.* 5:131–146.
16. Bauer, R. K., and A. Balter. 1979. A method of avoiding wavelength-dependent errors in decay-time measurements. *Optics Communications.* 28:91–95.
17. Rayner, D. M., A. E. McKinnon, and A. C. Szabo. 1977. Correction of instrumental time response variation with wavelength in fluorescence lifetime determinations in the ultraviolet region. *Rev. Sci. Instrum.* 48:1050–1054.
18. Rayner, D. M., A. E. McKinnon, A. G. Szabo, and P. A. Hackett. 1974. Confidence in fluorescence lifetime determinations: A ratio correction for the photomultiplier time response variation with wavelength. *Can. J. Chem.* 54:3256–3259.